Smooth Muscle Myosin Light Chain Kinase, Supramolecular Organization, Modulation of Activity, and Related Conformational Changes

Anatoly M. Filenko,[#] Valentina M. Danilova,[#] and Apolinary Sobieszek[*]
[*]Institute of Molecular Biology, Austrian Academy of Sciences, Salzburg, Austria, and [#]Institute of Physiology, Taras Shevchenko Kiev University, Kiev 252033, Ukraine

ABSTRACT It has recently been suggested that activation of smooth muscle myosin light chain kinase (MLCK) can be modulated by formation of supramolecular structures (Sobieszek, A. 1991. Regulation of smooth muscle myosin light chain kinase. Allosteric effects and co-operative activation by CaM. *J. Mol. Biol.* 220:947–957). The present light scattering data demonstrate that the inactive (calmodulin-free) MLCK apoenzyme exists in solution as a mixture of oligomeric (2% by weight), dimeric (53%), and monomeric (45%) species at physiological ionic strength (160 mM salt). These long-living assemblies, the lifetime of which was measured by minutes, were in equilibrium with each other. The most likely form of the oligomer was a spiral-like hexamer, the dimensions of which fit very well the helical structure of self-assembled myosin filaments (Sobieszek, A. 1972. Cross-bridges on self-assembled smooth muscle myosin filaments. *J. Mol. Biol.* 70:741–744). After activation of the kinase by calmodulin (CaM) we could not detect any appreciable changes in the distribution of the kinase species either when the kinase was saturated with CaM or when its molar concentration exceeded that of CaM. Our fluorescent measurements suggest that the earlier observed inhibition of kinase at substoichiometric amounts of CaM (Sobieszek, A., A. Strobl, B. Ortner, and E. Babiychuk. 1993. Ca^{2+}-calmodulin-dependent modification of smooth-muscle myosin light chain kinase leading to its co-operative activation by calmodulin. *Biochem. J.* 295:405–411) is associated with slow conformational change(s) of the activated (CaM-bound) kinase molecules. Such conformational rearrangements also took place with equimolar kinase to CaM; however, in this case there was no decrease in MLCK activity. The nature of these conformational changes, which are accompanied by reduction of the kinase for CaM affinity, is discussed.

INTRODUCTION

Myosin light chain kinase (MLCK) is a key regulatory enzyme of the smooth muscle. Upon cell stimulation, when intracellular Ca^{2+} increases from ~0.14 μM to 0.5–0.7 μM or more (Williams and Fay, 1986), Ca^{2+} ions are chelated by calmodulin (CaM). After saturation of CaM by Ca^{2+} its affinity toward kinase increases some 10^6-fold and an active CaM-MLCK complex is formed. The activated kinase species (Ca^{2+}-CaM-MLCK) phosphorylates the regulatory light chain (RLC) of myosin at its residue Ser-19. Phosphorylated myosin heads may enter into cyclic interaction with actin filaments and, using ATP energy, enable contraction or shortening of the muscle cells (Kamm and Stull, 1985; Marston, 1982; Adelstein and Eisenberg 1980; Small and Sobieszek, 1980). Another regulatory enzyme, myosin light chain phosphatase (MLCP), inactivates myosin by dephosphorylation bringing about relaxation (Hartshorne and Kawamura, 1992).

MLCK is fully inactive in the absence of Ca^{2+} and/or CaM. A large number of studies (Ito et al., 1991; Kemp et al., 1987; Pearson et al., 1988; Pearson et al., 1991) suggest that the kinase is inhibited by a pseudosubstrate domain which has amino acid sequence homological to the phosphorylation site (residues 1–19) of the RLC. The CaM-binding site of the kinase is a part of the pseudosubstrate domain and hence, upon CaM binding, this domain is removed from the active site and the enzyme becomes active. This concept of MLCK regulation has been confirmed in a number of studies on MLCK fragments (Pearson et al., 1988; Pearson et al., 1991). Correspondingly, on one hand, the kinase with a partly removed CaM binding site could not be transferred into an active state and, on the other hand, kinase fragments with a removed pseudosubstrate domain exhibit full activity in the absence of CaM and Ca^{2+}. This activation model has also been confirmed by studies with synthetic peptides analogous, in their sequences, to CaM binding sites. They inhibited the activity of MLCK (Kemp et al., 1987; Kennelly et al., 1987). Besides the autoinhibition, additional conformational change(s) of kinase may take place and this is evidenced by studies involving the binding of CaM mutants by the kinase apoenzyme (Van-Bercum and Means, 1991).

An important feature of the pseudosubstrate domain is that it contains a high number of basic residues that can be aligned with those of the N-terminal portion of the regulatory light chain as needed for the autoinhibition (Ikebe et al., 1987, 1989; Kemp et al., 1987; Pearson et al., 1988). This has been confirmed by studies with synthetic peptides, which are analogous in their sequences to CaM binding sites. They inhibited the activity of MLCK (Kemp et al., 1987; Kennelly et al., 1987), and two hydrophobic residues within this domain were shown by NMR spectroscopy to be essential for their binding to the kinase, and therefore its

Received for publication 7 August 1996 and in final form 2 June 1997.

Address reprint requests to Apolinary Sobieszek, Institute of Molecular Biology, Austrian Academy of Sciences, Billrothstrasse 11, A-5020 Salzburg, Austria. Tel.: 43-662-63961-14; Fax: 43-662-63961-40; E-mail: asobieszek@oeaw.ac.at.

0006-3495/97/09/1593/14 $2.00

activation by CaM (Ikura et al., 1992; Meador et al., 1992). Very recent studies, however, indicate that hydrophobic residues outside this domain, namely Tyr-794–Met-795–Ala-796, are critical for the autoinhibition (Tanaka et al., 1995) and not these basic residues. This explains why some of the previous site-directed mutagenesis experiments (Knighton et al., 1992; Means et al., 1991; Yano et al., 1993) were inconsistent with the autoinhibition model and indicates that additional conformational change(s) of kinase may also be necessary for the intrasteric inhibition.

Our earlier in vitro studies show that when kinase is preincubated (before adding ATP) with substoichiometric amounts of Ca^{2+}-CaM, its activity may decrease several-fold. We suggested that this modification might be related to changes in the supramolecular organization of MLCK complexes (Sobieszek et al., 1993). These modification(s) may take place in vivo because they resulted in an increase in the cooperativity of the activation of MLCK by CaM. The aim of this work was to shed more light on this activation process and to characterize MLCK supramolecular organization. Using light scattering and fluorescence methods we could demonstrate that smooth muscle MLCK formed oligomers and that the inhibition or its cooperative activation by CaM did result from additional conformational change(s) within its molecular or supramolecular organization.

MATERIALS AND METHODS

Protein preparation

MLCK and CaM were purified from turkey gizzard as described elsewhere (Sobieszek and Barylko, 1984; Sobieszek, 1991; Sobieszek et al., 1993). Their concentrations were determined using absorption coefficients of $A_{278}^{1\%} = 11.4$ and $A_{278}^{1\%} = 1.0$, respectively, for the kinase and CaM (Adelstein and Klee, 1981).

Myosin and its 20-kDa RLC were used as MLCK substrates. Myosin was purified from freshly extracted turkey gizzard actomyosin (Sobieszek and Bremel, 1975) by $(NH_4)_2SO_4$ fractionation (Sobieszek, 1985, 1994) and stored at −70°C. The RLC was isolated by the method of Perrie and Perry (1970) and purified as previously described (Sobieszek, 1988). Concentration of myosin and its light chain were measured by the biuret method (Gornall et al., 1949).

Activity measurements

Phosphorylation rate measurements were carried out at 25°C in the buffer AA of the following composition (mM/l): KCl, 60; $MgCl_2$, 2; dithioerythritol, 0.5; imidazole, 10; with pH adjusted to 7.5 at 4°C. Unless otherwise stated, 100 mM NaCl were added to this buffer during all measurements. All other experimental details were as described previously (Sobieszek, 1991; Sobieszek et al., 1993) or as given in the corresponding figure legends.

Photon correlation spectroscopy

The MLCK solutions used for photon correlation spectroscopy (PCS) were passed through a Millipore filter (0.22 μm; Bedford, MA) to remove dust particles. The apparatus used in these measurements included a helium-neon laser (Spectrophysics, Santa Barbara, CA) operating at a wavelength of 632.8 nm with a 50 mW light source, goniometer ALV/SP-86 (Optimation GmbH, Munchen, Germany), and correlator K7032 (Malvern Instruments Ltd., Spring Lane South, UK). During the measurements, light scattered by the solution was collected at a right angle to the laser beam's direction. Analysis of the data was carried out on an IBM PC according to the regularization procedure described elsewhere (Braginskaya et al., 1983). Use of the PCS data together with the regularization mathematical program made it possible to obtain information about effective hydrodynamic diameters of the particles and their relative distribution.

Multi-angle laser light scattering

Continuous distribution of weight average molecular weights (M_w) and root mean square (RMS) radii of MLCK were obtained in the course of MLCK elution from chromatographic columns connected to a multi-angle laser light scattering instrument. For this purpose a multi-angle laser light scattering photometer (Wyatt Technology Corporation, Santa Barbara, CA) was used connected to a standard fast liquid protein chromatography (FPLC) station (Pharmacia, Uppsala, Sweden). The Wyatt Dawn model F photometer used included a 632.8-nm laser as a light source and collected analog signals from 15 light-sensitive photodiodes placed at different angles to the incident laser beam. They were sent to an IBM PC where the signals were digitized and processed. The 16th channel was used for the signal from a mass-sensitive UV detector (280 nm) of the FPLC station placed between the column and the photometer flow cell. The FPLC station included: a GP-250 controller, P-500 high precision pumps, a V-7 valve with 500 ml loop, an REC-102 recorder, a UV-1 ultraviolet monitor, and a column. Connecting tubing between column and the Dawn instrument were kept as short as possible to minimize delays. These were 0.10 ml between the column and the UV-monitor and 0.16 ml between the UV-monitor and the Dawn cell. Gel-filtration, CaM-affinity, and ion-exchange columns were used in our experiments. A gel filtration column (0.6×28 cm) was packed with Sephacryl S-300; a strong cation exchanger with SP-Sepharose FF (0.6×6 cm) and an anion exchanger with DEAE-Sepharose 6B-CL (0.6×6 cm); all were from Pharmacia (Uppsala, Sweden). The CaM-affinity column (0.5×4 cm) was prepared from purified turkey gizzard CaM and CN-Br-activated Sepharose 4B-CL as recommended by the manufacturer. Before chromatography, all solutions were carefully degassed and filtered through a Millipore 0.22 μm filter. A number of experiments were carried out without the columns by a direct injection of MLCK into the Dawn flow cell using a syringe equipped with a Millipore 0.22 μm filter.

Light scattering data were analyzed on an IBM PC using Wyatt ASTRA software. In the calculations we assumed that the specific refractive index increment was $dn/dc = 0.17$ ml/g and that the second viral coefficient A_2 was equal to 0.

Fluorescence methods

For detection of MLCK conformational changes three fluorescence approaches were used. In the first, 9-antroylcholin (9AC) was applied as a fluorescent probe because it binds specifically to smooth muscle MLCK (Malencik et al., 1982). The 9AC fluorescence was excited at 366 nm and registered at 462 nm. Measurements were carried out using a spectrofluorimeter MPF-3L (Hitachi Ltd., Tokyo, Japan).

In the second approach, MLCK intrinsic (tryptophanyl) fluorescence was measured. To register small changes of MLCK intrinsic fluorescence during preincubation time a spectrophotometer M-40 (Carl Zeiss, Jena, Germany) was used at an excitation wavelength of 280 nm. This instrument measures the ratio of fluorescence signals in two channels, one of which was used as the reference. The excitation component in the total fluorescence emission was cut off by a filter which transmitted only emissions >300 nm. At the beginning of the measurements the same solution, containing MLCK, CaM, and EGTA, was poured into both cells placed in the main and reference channels. Subsequently the kinase in the main channel cell was activated by adding a very small volume of $CaCl_2$ solution (0.1 mM final free concentration), and changes in the intrinsic fluorescence were recorded.

In the third approach, the fluorescence anisotropy of MLCK-CaM complexes was measured using CaM fluorescently labeled with dansyl chloride. These experiments were carried out in Dr. Tobias Meyer's laboratory at Duke University (Durham, NC) using the instrument described previously (Meyer et al., 1992). That instrument makes it possible to measure fluorescence polarization of proteins in solution at equilibrium. The probe fluorescence was excited by polarized light at 330 nm and anisotropy was registered at 510 nm. As a consequence, the imidazole in the AA buffer was replaced by HEPES. Other details are given in the corresponding figure legends.

RESULTS

Effect of MLCK preincubation on its activation by CaM

It has been shown earlier that under some conditions smooth muscle MLCK is activated by CaM with positive cooperativity and that this cooperativity was not observed for activation of CaM by kinase (Sobieszek, 1991). We have extended this type of experiments and established that the cooperativity decreased significantly upon reduction of salt concentration (data not shown). Therefore, the degree of positive cooperativity was even higher at physiologically relevant ionic conditions in comparison to the conditions used previously. This is most readily illustrated by the relationship between activity and MLCK concentration measured at a constant CaM level (Fig. 1, *solid diamonds*). This relationship demonstrates that MLCK activity increased steeply and uncooperatively until the CaM present became saturated by the kinase. Further increase in the apoenzyme concentration resulted in reduction of this activity with almost complete inhibition at ~4- to 6-fold molar excess of the apoenzyme over CaM. The extent of this inhibition is a measure of the cooperativity because

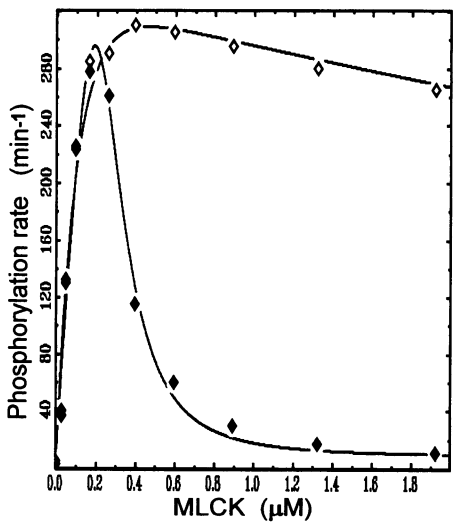

FIGURE 1 Inhibitory effect of smooth muscle MLCK. After preincubation of the kinase with substoichiometric levels of CaM its activity was inhibited (◆) while without preincubation (the phosphorylation reaction initiated by adding ATP together with CaM) no inhibition was observed (◇). MLCK activity was measured as function of its concentration at a constant CaM concentration of 0.16 μM. Isolated RLC was used as the substrate, and preincubation time was 15 min. The kinase and CaM preparations used in this and subsequent figures were from turkey gizzard. Unless otherwise stated the buffer used was AA+100 mM NaCl.

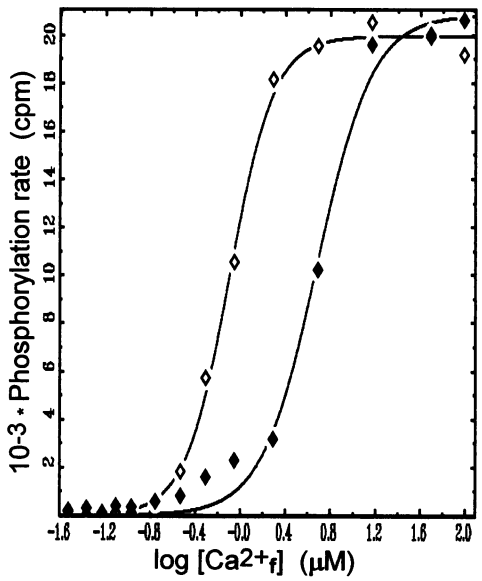

FIGURE 2 Effect of preincubation of CaM-MLCK complex on its activation by Ca^{2+}. The rates measured without the preincubation (◇) were obtained in 30 s assays while those with the preincubation (◆) required 5 min. Note that aside from this 10-fold rate difference the activation of the preincubated CaM-MLCK complex also required a 40-fold higher Ca^{2+} concentration. Filamentous myosin (50 μM) was used as the substrate and concentrations of MLCK and of CaM were 1.5 and 0.25 μM respectively. Ca^{2+} concentrations were buffered with a 2.5 mM Ca/EGTA buffer system and were calculated using an apparent binding constant (K_{app}) of EGTA for Ca^{2+} of $K_{app} = 1.470 \cdot 10^{-7}$ M.

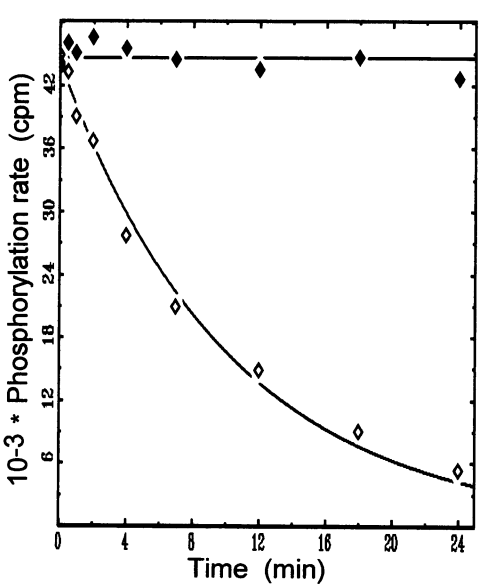

FIGURE 3 Dependence of CaM-MLCK inhibition on preincubation time at low (◇) and at high (◆) concentrations. Note that the inhibition was observed after preincubation at low but not at 10-times higher concentrations. The final concentrations of MLCK (150 nM) and CaM (3 μM) were exactly the same. Filamentous myosin (40 μM) was used as the substrate.

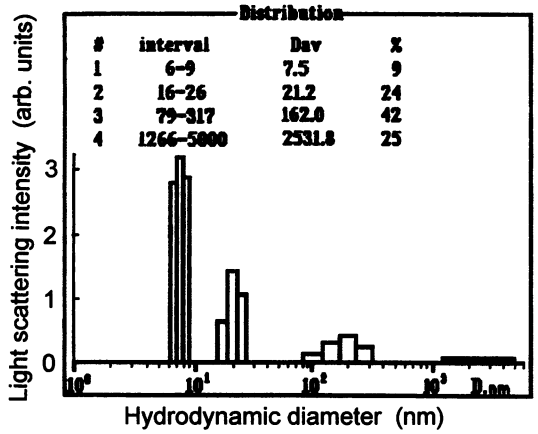

FIGURE 4 Particle size distribution of MLCK obtained by PCS method. For convenience, the hydrodynamic diameter of the particles D_{av} (in nm) is plotted using logarithmic scale. Data shown here represent one experiment. The remaining data of this type are gathered in Table 1. MLCK concentration was 4.9 μM.

after saturation the activity should remain constant, and it depends only on the concentration of the active CaM-MLCK complexes. When the phosphorylation reaction was initiated with ATP and CaM (no preincubation with CaM), no inhibition was observed and the activation was hyperbolic (Fig. 1, *open diamonds*). Thus, the inhibition resulted from preincubation of the MLCK with substoichiometric amounts of Ca^{2+}-CaM before the initiation of the phosphorylation reaction. We call this phenomenon inhibitory effect because it involved significant reduction of the rate (V_m) and of the apparent affinity of CaM-MLCK complex for free calcium (Fig. 2) but not of the overall affinity of MLCK for CaM (see Sobieszek et al., 1993).

It was apparent that during the preincubation time the kinase underwent some Ca^{2+}-CaM dependent modification(s). The time range during which such changes were taking place was established in different types of experiments. In this case the MLCK activity was measured as a function of the preincubation time under conditions when the inhibitory effect was optimal, i.e., at high and constant kinase-to-CaM molar ratio. As shown in Fig. 3, the kinase required 10 to 15 min (at 25°C) of preincubation with Ca^{2+}-CaM to undergo modification into the inhibitory state (*open diamonds*). If preincubation was carried out at high kinase concentration (5–10 μM), at the same final CaM and kinase concentrations, the inhibitory effect was not observed (Fig. 3, *solid diamonds*). Thus, it is possible that oligomeric-type transformation(s) were involved in the ob-

TABLE 1 Average hydrodynamic diameters (D_{av}) of the MLCK species and their contributions (%) to light scattering at different kinase to CaM ratios

Experiment No.	Measurement No.	$D_{av}(3)$	%	$D_{av}(2)$	%	$D_{av}(1)$	%
1				4.9 μM MLCK, without CaM			
	1	162.0	56	21.2	32	7.5	12
	2	185.4	51	25.8	32	10.1	17
	3	172.4	45	18.6	41	8.2	14
2				4.9 μM MLCK, 0.2 mM EGTA, 12.7 μM CaM			
	1	155.4	51	19.7	38	8.8	11
	2	157.6	51	18.6	39	7.1	10
	3	126.5	49	21.5	36	6.7	15
				+0.4 mM $CaCl_2$			
	4	151.3	54	16.9	34	8.9	12
	5	155.7	59	27.1	35	8.5	6
	6	182.2	50	16.6	37	9.2	13
	7	154.5	47	20.3	45	11.3	8
3				4.9 μM MLCK, 0.2 mM EGTA, 1.5 μM CaM			
	1	161.7	62	16.9	32	6.4	6
	2	151.2	53	24.1	37	9.0	10
	3	140.5	50	18.3	36	7.8	14
				+0.4 mM $CaCl_2$			
	4	124.6	46	22.7	42	8.2	12
	5	159.0	57	17.9	34	9.9	7
	6	157.0	55	16.3	37	8.9	8
	7	193.8	53	21.5	40	8.9	7
Arithmetic average		158.8	52.3	20.2	36.9	8.8	10.8

$D_{av}(1)$, $D_{av}(2)$, and $D_{av}(3)$ are average hydrodynamic diameters of MLCK monomer, dimer, and oligomer, respectively. Buffer composition was as given in Materials and Methods. Duration of each measurement was 2 min and measurements 1–3 and 4–7 were carried out without interruption using an automatic regime, except for the indicated $CaCl_2$ injection and mixing that required ~40 s. The percent contributions into the MLCK light scattering were corrected for the scattering introduced by dust particles.

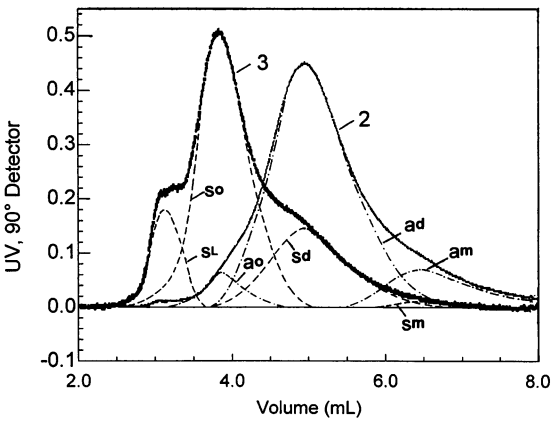

FIGURE 5 Elution and light scattering profiles obtained during MLCK gel filtration and their separation into single peak contributions. A short Sephacryl S-300 column was connected to a UV-monitor and DAWN Wyatt instrument. For more details see Materials and Methods. Trace 2 corresponds to the UV-absorption and curve 3 to the light scattering at 90°. Absorption monopeaks were designated "a^i" and light scattering "s^i" where index "o" represents the oligomer, "d" the dimer, "m" the monomer, and where "S^L" corresponds to large MLCK aggregates. 0.56 mg (500 μl) of the kinase was applied to the column. Unless otherwise stated in this and the following figures flow rate was 0.25 ml/min.

served modification. To test this hypothesis it was necessary to characterize MLCK supramolecular organization, and light scattering is the most suitable method for this purpose.

Equilibrium distribution of different MLCK species in solution

As a first step of MLCK characterization by light scattering methods we evaluated its species size distribution using photon correlation spectroscopy (PCS) because that method does not introduce perturbation into the protein studied (Nicoli et al., 1992). It must be noted that the regularization software used in this method provides sizes for the spherical-shaped particles, so that the hydrodynamic sizes obtained are close to their true sizes only in the case of globular proteins. For other proteins, the shape of which differs strongly from a sphere, the hydrodynamic sizes obtained are rather conditional values. This fully applies to MLCK, because it has been concluded that the kinase molecule is a rod-shape of 50 nm in length and 2.2 nm in diameter (Ausio et al., 1992).

Fig. 4 shows a typical pattern of such distribution carried out for a kinase solution at 4.9 μM concentration (all the data obtained are given in Table 1). Scattering in the range of 1266–5000 nm must be due to the presence of a small quantity of dust particles that are very difficult to remove completely by standard filtration. The other scattering components were related to kinase assemblies, and this was obvious from dependence of their scattering on the scattering angle (data not shown).

TABLE 2 Contributions of the MLCK species to the elution profiles obtained from the S-300 column

Kinase species	Oligomer	Dimer	Monomer
Scattering monopeak area, s^{i*}	122.0	53.6	3.0
UV absorption monopeak area, a^{i*}	11.0	170.6	27.7
The amount in eluate, wt %#	5.26	81.51	13.23
Relative contribution to light scattering (δ^i)§	35.3	1.0	0.345

*Areas of individual peaks (see Fig. 5) were estimated by weighing. Index "i" corresponds to o-oligomer, d-dimer, or m-monomer.
#This value was estimated from UV absorption of the individual peaks (a^i) assuming that their total area is 100%.
§This parameter was calculated from the following expression: δ^i = (area s^i/area a^i)/(area s^d/area a^d); it represents light scattering of MLCK oligomer and monomer relative to dimer assuming that wt % concentrations of all three species are equal.

The particles of D_{av} = 7.5 nm in the 6- to 9-nm range (Fig. 4) were identified as MLCK monomers. They possibly included some smaller size particles corresponding to the large kinase proteolytic fragments. The length of the kinase dimer should be twice that of the monomer (Ausio et al., 1992) and correspondingly we observed particles with D_{av} = 21.2 nm in the 16–26-nm range. Particles with D_{av} = 162 nm in the 79–317-nm range must correspond to the kinase oligomer species. More accurate D_{av} values, used in further calculations, are given in Table 1. They were arithmetic averages of all the experimental data.

Table 1 shows the data obtained by the PCS method for MLCK solution with and without CaM at its different molar ratios to MLCK before and after formation of the active complex. Owing to the small size of the CaM molecules and their low concentration, the contribution of the light scattering from CaM was negligible under our experimental conditions. As indicated above, the inhibition of the kinase (5–10 min following addition of Ca^{2+}-CaM) was not observed at high kinase concentrations, so that we restricted our measurements to relatively low kinase concentrations and rather short times (2 min). These conditions were, however, far from being optimal for the PCS method and, as

TABLE 3 Contribution of the MLCK species at equilibrium

Kinase species	Oligomer	Dimer	Monomer
Contribution to light scattering (I^i) at equilibrium, %*	52.3	36.9	10.8
Relative contribution to light scattering, $\delta^{i\#}$	35.3	1.0	0.345
The amount in solution (B^i) at equilibrium, wt %§	2.13	52.95	44.92

*Data taken from Table 1 represent the arithmetic average of 17 experiments. For values of the index "i" see Table 2.
#Data taken from Table 2.
§Concentrations of different MLCK species at equilibrium in wt % were calculated from the following expression: $B^i = [(I^i/\delta^i):(I^o/\delta^o + I^d/\delta^d + I^m/\delta^m)] \times 100$.

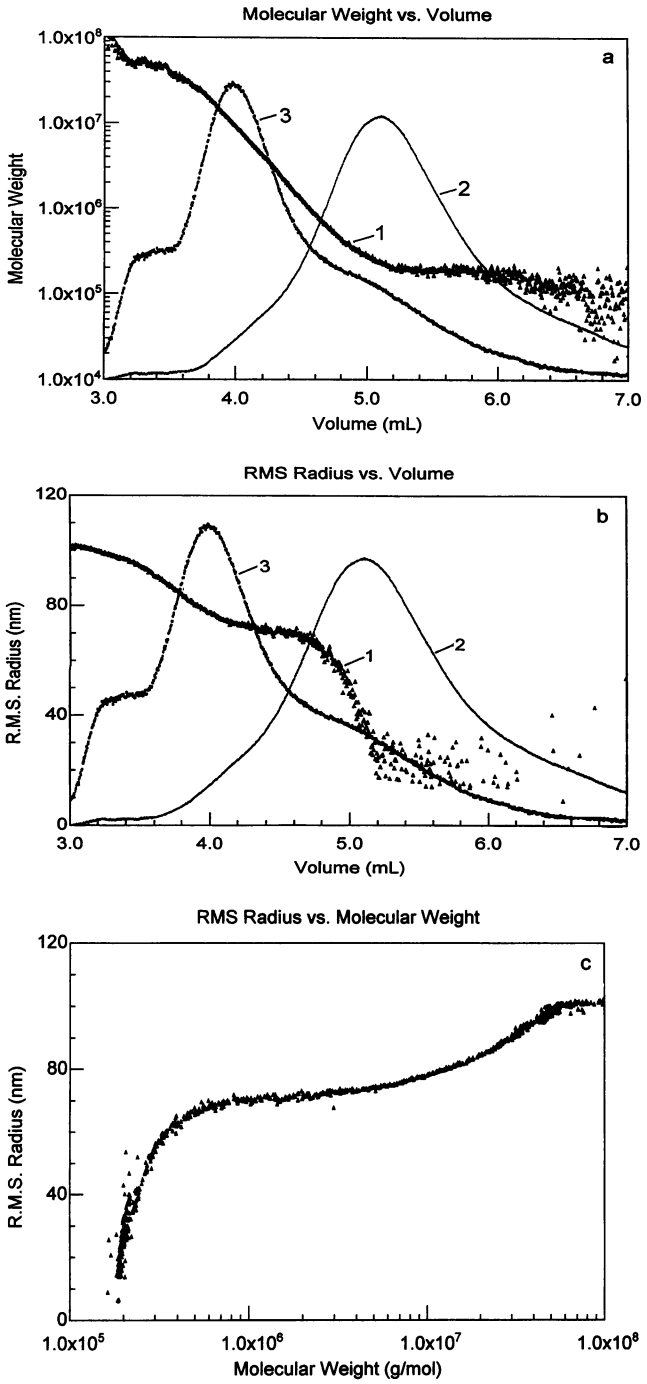

FIGURE 6 Distribution of MLCK M_ws (*a*; curve 1) and RMS radii (*b*; curve 1) as well as the relationship between them (*c*) during elution of MLCK from the S-300 column. For convenience the elution (trace 2) and light scattering (curve 3) profiles were also included (see Fig. 5).

a consequence, the spread in data is rather large (Table 1). Nevertheless, the data presented in Table 1 indicate that Ca^{2+}-CaM binding to kinase at both high or low MLCK-to-CaM ratios following 8 min of preincubation had practically no influence on both the size of the enzyme species and their relative concentrations.

TABLE 4 Molecular weight and RMS radius of MLCK oligomer and dimer

Kinase species	Interval on elution curve (ml)	Molecular weight	RMS radius (nm)
Oligomer	3.7–3.8	2.00×10^7	80
Dimer	5.2–5.7	2.00×10^5	22

Characterization of MLCK species during chromatographic elutions

The gel filtration column used was too short, and the flow rate too fast to produce complete separation of the MLCK species. Its main function was to produce a continuous distribution of the kinase concentrations, besides removing the troublesome dust particles. Fig. 5 shows characteristic elution profiles obtained from the FPLC UV-monitor (trace 2) and the continuous light scattering data recorded by a computer collecting data from the Wyatt DAWN photometer (curve 3). For a monodisperse system these curves should coincide within some constant factor (Wyatt, 1993). In our measurements they exhibited a complex shape as a result of overlapping of several elution peaks. Aided by similar plots obtained for monodisperse systems (polystyrol of 30 and 200 kDa and bovine serum albumin) we decomposed these plots into the individual peak contributions (Fig. 5). The main requirement of this procedure is that the sum of the monopeaks should give the original elution plot and that the related light scattering and UV-absorption monopeaks should coincide within a constant factor.

As shown in Fig. 5, the UV-absorption profile (trace 2) was decomposed into three overlapping monopeaks with maxima at 3.8 ml (peak a^o), 5.0 ml (peak a^d), and 6.5 ml (peak a^m). From their elution positions these peaks must be related to the light scattering peaks of the oligomeric (s^o),

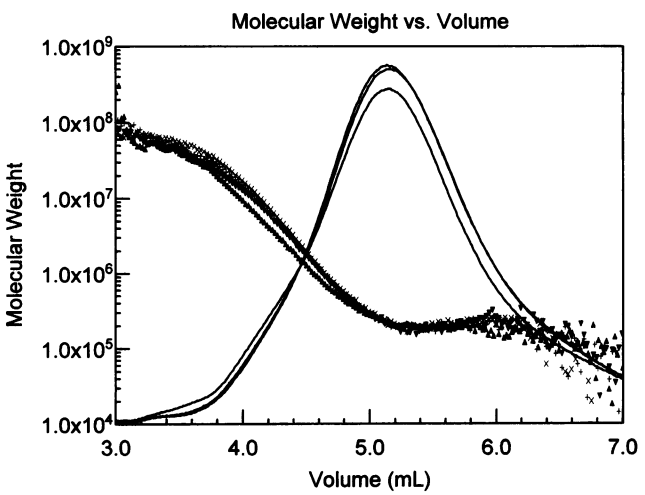

FIGURE 7 Elution profiles and M_w distributions obtained during the S-300 column elution at different MLCK to CaM molar ratios; 10:1 (x—x), 5:1 (+—+), 1:1.5 (▲—▲) and without CaM (▼—▼). In all experiments 0.56 mg (500 μl) of the kinase was applied and 0.1 mM $CaCl_2$ was added to the elution buffer.

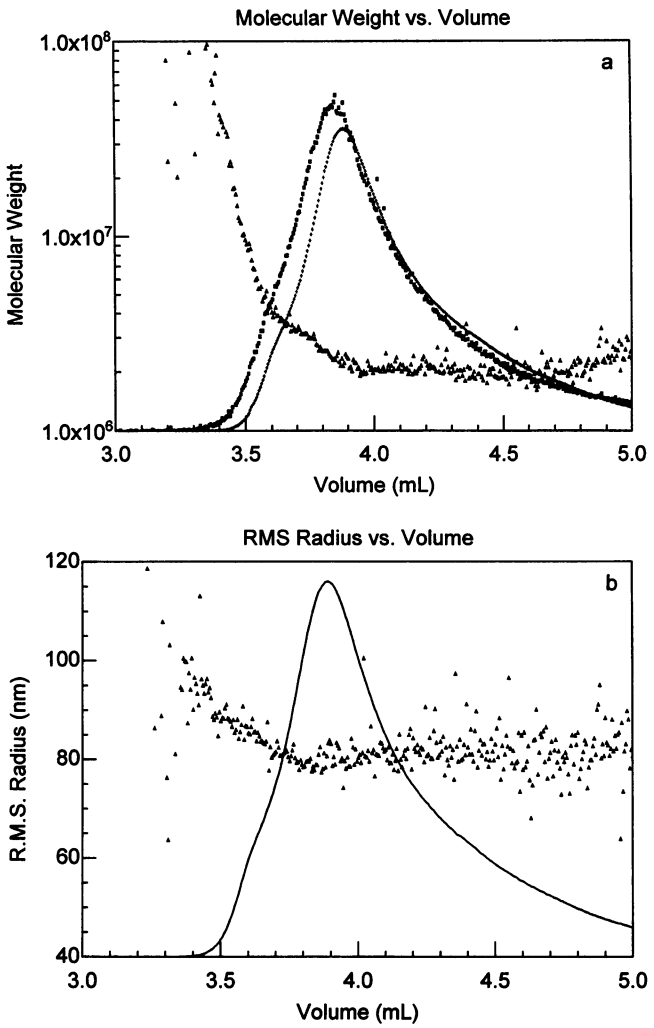

FIGURE 8 MLCK M_w (*a*) and RMS radius (*b*) distribution during elution from the CM-affinity column (▲). MLCK (0.53 mg) was applied to the column. During MLCK application the buffer contained 0.1mM $CaCl_2$ and this was replaced by 2 mM EGTA during elution. Flow rate was 0.15 ml/min. For the convenience, elution profile (*b*, —) was also included. Note that in (*a*) the light scattering (■, 90° detector) and elution profile (×) nearly coincide which indicates the presence of an essentially single MLCK species. Note also that in (*b*) an approximately constant RMS radius of ~80 nm was observed along an elution profile also indicating the presence of a single oligomeric MLCK form.

dimeric (s^d), and monomeric (s^m) kinase species. The peak s^L clearly resulted from light scattering of the large kinase aggregates or the column "debris" because it was eluted in the void volume of the column. Clearly seen in Fig. 5 are small elution intervals where the monopeaks do not overlap. They correspond to the individual contribution of kinase oligomer (3.7–3.8 ml), dimer (5.1–5.6 ml), and monomer (6.8–7.5 ml). These three short elution intervals were used for calculation of relative contributions of the individual kinase species within the light scattering plots. However, more accurate data of this type were also obtained from calculations which included the corresponding monopeak area ratios (Table 2).

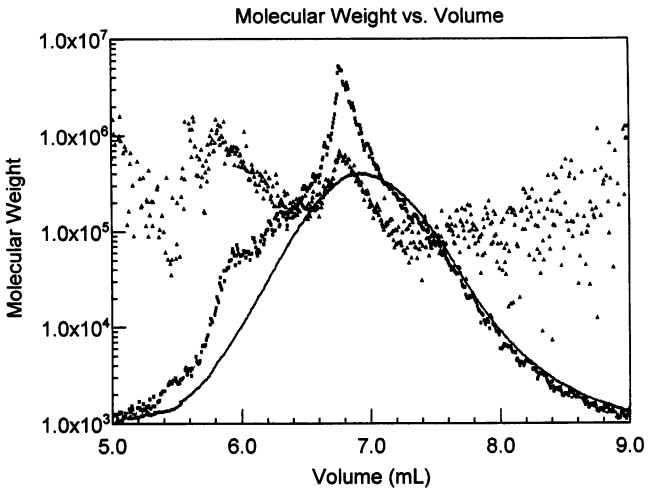

FIGURE 9 Elution profile (—), M_w distribution (▲), and light scattering (■) obtained during MLCK elution from a strong cation exchange column. Note that essentially monomeric kinase (0.56 mg applied) eluted from the column. The column was eluted with a 60 to 200 mM NaCl gradient added to our AA buffer.

Table 2 shows that at the same concentrations (in wt %) light scattering of the oligomer was 35 times larger than that of the dimer; at the same time the monomer scattering was ~3 times smaller than that of the dimer. The large contribution of the oligomers into the light scattering plots is also clear from Fig. 5 where, at the exit from the column, the weight contributions of the kinase oligomer, dimer, and monomer were 5.3, 81.5, and 13.2 wt %, respectively. These individual contributions together with our PCS data obtained for the individual kinase species at equilibrium (Table 1) as well as the relative contributions of the three species into light scattering (Table 2) made it possible to calculate the relative content of the oligomers, dimers, and monomers at equilibrium (Table 3).

M_w and RMS radius distribution

Fig. 6 shows dependencies of the weight average molecular weight (M_w) and root mean square (RMS) radius on the elution coordinate calculated by using Wyatt ASTRA software. The data in the elution interval from 6.3 to 7.0 ml have less reliability due to poor light scattering, but they nevertheless indicate the presence of monomers (Fig. 6 *a*) from the known 110-kDa molecular weight of the kinase. Owing to the overlapping between the oligomer and the dimer peaks, the curves had a characteristic half-bell-like shape and the calculations obtained for each elution slice in the 3-to-5.2-ml interval did not permit evaluation of the species-specific M_w and RMS radii values. The characteristic feature of these curves was rapid growth by a factor of 100 of the M_w in parallel to the decrease in the elution coordinate within the interval of 3.8 to 5.2 ml (Fig. 6 *a*). This was accompanied by a relatively small increase in the RMS radius from 22 to 80 nm (Fig. 6 *b*). This points to the

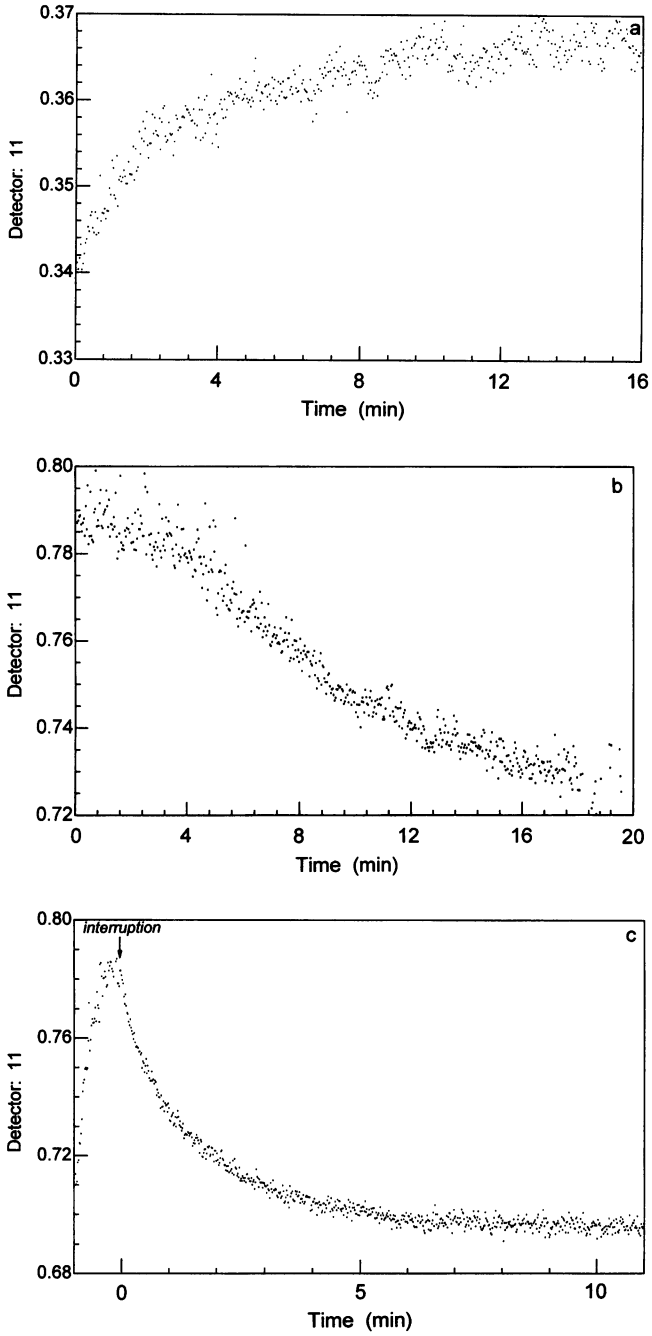

FIGURE 10 Time dependent changes of MLCK light scattering after interruption of the elution from the S-300 column at the position of the dimers (*a*), of the oligomers (*b*), and of the oligomers eluted from the CaM-affinity column (*c*). Light scattering (arbitrary units) was measured at 90° (Detector 11) to the incident beam. Note the increase in the scattering intensity in (*a*) and its decrease in (*b*) and (*c*). For more details see text.

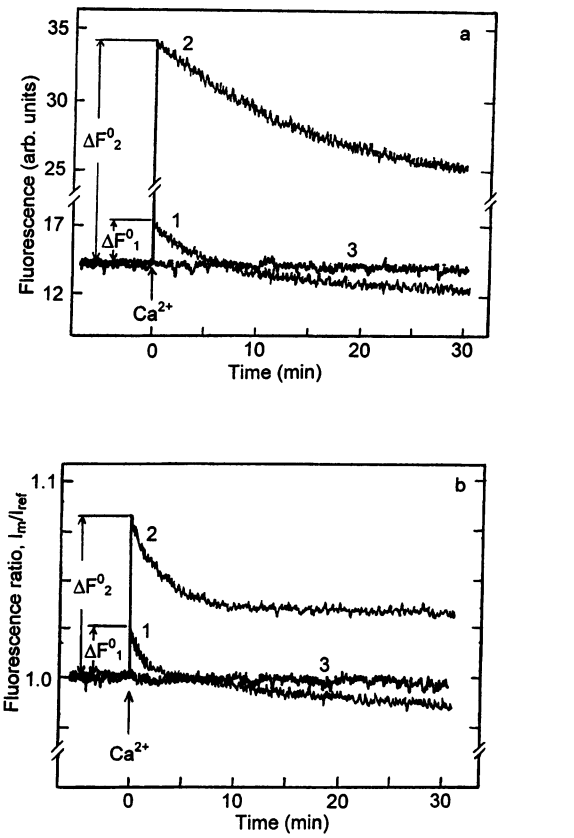

FIGURE 11 Time-dependent decrease of MLCK fluorescence following formation of the active Ca^{2+}-CaM-MLCK complexes. Their formation was triggered by injection of 0.4 mM $CaCl_2$ into the buffer. Initial level of the fluorescence before $CaCl_2$ injection is shown on the left from 0 time point. (*a*) Fluorescence of the 9AC probe bound to MLCK (1.2 μM); trace 2: MLCK to CaM molar ratio of 1 to 4; trace 1: 1 to 0.33; trace 3: control. 9AC concentration was 20 μM and the cuvette temperature was 15°C; excitation at 355 nm, fluorescence registration at 462 nm. (*b*) Intrinsic (tryptophanyl) fluorescence of MLCK (1.1 μM); trace 2: MLCK to CaM molar ratio 1 to 3.4; trace 1: 1 to 0.37; trace 3: control. The cuvette temperature was 18°C and excitation wavelength 280 nm. Total MLCK fluorescence (not decomposed in spectrum) in the region of 300–600 nm was registered. Ratio of main channel emission (I_m) to reference one (I_{ref}) was measured in an automatic regime.

existence of kinase forms differing greatly in their molecular masses but exhibiting rather constant dimensions, a conclusion which was fully consistent with our electron microscope images of negatively stained MLCK preparations (data not shown). Our estimations of the MW and RMS radii of the kinase oligomer and the dimer (Table 4) are based on the elution intervals corresponding to the single kinase species (Fig. 5) and to the data shown in Fig. 6. As a result of poor light scattering this type of calculation was not possible for the monomer (see Fig. 6 *b*; 5–6-ml interval).

The data shown in Fig. 6 were obtained for inactive kinase apoenzyme (no CaM added). However, from the data obtained at different apoenzyme to CaM ratios it was clear that binding of CaM by kinase had little effect on distribution of M_w (Fig. 7) or on the RMS radius (data not shown) nor on the elution profiles (Fig. 7, *solid traces*).

M_w and RMS distribution during ionic-exchange and CaM-affinity chromatography

A number of experiments was carried out with other types of columns. Fig. 8 shows elution profiles and the M_w and

RMS radii distributions obtained from the CaM-affinity column. In the presence of Ca^{2+} ions, MLCK binds to CaM covalently linked to a column matrix and can be specifically eluted with a solution containing EGTA. As is clear from Fig. 8 *a* both elution profiles (UV-absorption: *small crosses*; light scattering: *solid squares*) nearly coincide, indicating that the eluate practically contained a single kinase species. The plot shown in Fig. 8 *b* suggests that this species corresponded to an oligomer with an RMS radius of ~80 nm, which was similar to that eluted during gel filtration. In contrast, the M_w of this oligomer was relatively constant (Fig. 8 *a*) with a value ~10 times less than the maximal M_w of the oligomer obtained during elution from the gel filtration column (Fig. 6).

Equally interesting were the MLCK elution profiles obtained from a strong cation-exchanger SP-Sepharose FF column. In this case the UV-absorption and light scattering peaks maxima also coincided (Fig. 9, compare *solid line* with *small solid squares*). It is also clear that this eluate contained only MLCK monomers (Fig. 9, *solid small triangles*). The sharp small peak at 220 kDa observed in the middle of the elution most likely represents the dimers formed during somewhat longer elution time due to binding of the kinase to top layers of the column. By contrast, the elution profiles obtained from an anion exchange DEAE-Sepharose 6B-CL indicated the presence of relatively high concentrations of the oligomers of a rather wide range of M_w (data not shown) similar to those obtained during the gel filtration experiments.

Elution-interruption experiments

As indicated in Materials and Methods, the delay volume between the columns' outlet and the Wyatt instrument cell makes ~0.26 ml. This means that at an elution rate of 0.25 ml/min there was ~1 min delay before light scattering measurements were made. We assumed that MLCK species separated by the columns remained practically unchanged during this time. The validity of this assumption was investigated in experiments in which the elution was interrupted or stopped at the required elution point. Fig. 10, *a* and *b* show experiments of this type with our gel filtration column with interruption at 5 and 4 ml, respectively. From Fig. 5 we know that at the 5-ml elution coordinate the kinase dimers predominated. Therefore, the changes of light scattering at this point made it possible to observe how the dimer reapproached a true equilibrium. Fig. 10 *a* shows that this process continues for about 10 min. We expected that the oligomer species should be even more stable. Indeed, interruption of the elution at 4 ml resulted in a slower time-dependent decrease of the light scattering (Fig. 10 *b*). At this point the eluate contained equal weight amounts of the dimers and oligomers, although the oligomer contribution to the light scattering predominated. These changes then reflected the transition of the oligomers to the kinase monomers and dimers. Even 20 min after the interruption, the light scattering intensity was only reduced by ~11%.

The interruption experiments were also done during elution from the CaM-affinity column. Although the oligomer in this eluate was characterized by 10-fold lower M_w (Fig. 8 *a*), its light scattering decreased much more (i.e., 17%) and approached a constant level within 5 to 10 min following the interruption (Fig. 10 *c*).

As indicated above, activation of MLCK by CaM did not lead to any significant changes of the elution profile (Fig. 7). This is an indirect indication that the wt % ratio of the three kinase species remained practically constant during the activation, which is in agreement with the LCS data. This was also independently confirmed in our experiments in which CaM and kinase were syringed directly into the photometer flow cell immediately after their mixing in the presence of Ca^{2+} (data not shown).

Fluorescence changes of 9AC-MLCK complex

Our light scattering data indicated that MLCK inhibition during the preincubation period could not be fully explained by quantitative redistribution of the kinase species, although the times involved were approximately the same. Therefore, the inhibitory effect must represent conformational change(s) of kinase molecules. To test this hypothesis we measured changes of fluorescence intensity and fluorescence anisotropy of MLCK under relevant conditions.

According to Malencik et al. (1982) fluorescent probe 9-antroylcholin (9AC) specifically binds to smooth muscle MLCK with a severalfold enhancement of its fluorescence. This enhancement again doubles upon CaM binding. As a consequence, the gain of 9AC fluorescence largely characterizes the affinity of Ca^{2+}-CaM for the apoenzyme. A reduction of the affinity must lead to a decrease of 9AC fluorescence. Figure 11 *a*) shows time-dependent changes in the 9AC fluorescence of the kinase following its activation, i.e., under conditions corresponding to our preincubation period. The activation was initiated by injection of Ca^{2+} to a solution containing MLCK, CaM, EGTA, and 9AC. The initial fluorescence level (before the Ca^{2+} injection) is shown to the left of the zero time at the abscissa. In the absence of Ca^{2+} and at constant 9AC concentration this level depended on the kinase concentration and was independent of the CaM concentration. The trace obtained at a 4-fold molar excess of the kinase over CaM (lower trace) shows a 20% increase upon the activation by Ca^{2+}. During preincubation this gain decreased reaching the initial level (*dotted line*) after ~6 min. This indicated that ~6 min were required for the active kinase complexes to disappear, and this correlates rather well with the time course of MLCK inhibition (Fig. 3).

Probe 9AC is known to bind mainly to the ATP binding site (Malencik et al., 1982) and its dissociation constants for active Ca^{2+}-CaM-MLCK complex and the apoenzyme are correspondingly 6.4 and 20 μM. Therefore, the decrease of Ca^{2+}-CaM to apoenzyme affinity should lead to a reduction of the 9AC affinity for the ATPase site and, as a conse-

quence, to a decrease in the active complex fluorescence up to the initial level. The observed fluorescence decrease below the initial level (during the preincubation period) indicates that an additional reduction in the affinity of the ATP-binding site for 9AC was taking place.

A parallel plot obtained at saturating levels of CaM relative to MLCK is shown by the upper trace in Fig. 11 *a*. In this case, the concentration of the active complexes was 4-times higher than in the preceding experiment (lower trace). Thus, the corresponding fluorescence gain (ΔF_2°) was several times greater. The fluorescence intensity decrease observed during the preincubation time was much lower (~10%). This indicates that similar (although much slower) affinity modifications were also taking place for CaM-MLCK complexes in this case. Activity measurements (Babiychuk et al., 1995) showed that under these conditions there is similar, although slower, reduction in the kinase activity.

Changes of the intrinsic fluorescence of MLCK

The binding of Ca^{2+}-CaM to smooth muscle MLCK is known to cause a shift of this protein intrinsic fluorescence peak from 331 to 327 nm and a 7% increase in quantum yield (Malencik et al., 1982). CaM does not contribute to the fluorescence because it has no tryptophanyl residues. We observed intrinsic fluorescence changes during MLCK activation (Fig. 11 *b*) similar to the probe fluorescence (Fig. 11 *a*). However, at a 3-fold molar excess of the kinase over CaM, the fluorescence gain at zero time was rather small (~2%) because only one-third of the kinase molecules were activated. This gain decreased to the initial level after ~5 min (Fig. 11 *b*, lower trace), which correlated with kinase inactivation (see Fig. 3). When MLCK was saturated with CaM (upper trace) the gain was ~6% and we observed a similar decrease in the fluorescence of the activated kinase, again with the fluorescence not decreasing below the initial level (Fig. 11 *b*, upper trace). Hence, the pattern of intrinsic fluorescence after kinase activation was analogous to the pattern of 9AC fluorescence.

Fluorescence anisotropy

To evaluate directly the affinity of CaM for the kinase at their different molar ratios we also measured fluorescence anisotropy of CaM labeled with dansyl chloride (CaM_d; Fig. 12). Owing to sharp restriction of the CaM_d rotational motility after its binding to MLCK the bound probe fluorescence anisotropy of such a solution increased from 0.06 to 0.14. When great molar excess of unlabeled CaM was subsequently added to this solution it replaced the CaM_d bound to MLCK. The anisotropy decay is used as a measure of the "off" rate constant for departure of CaM from the kinase. With this method we first established that ATP presence had no effect on the affinity of MLCK for CaM

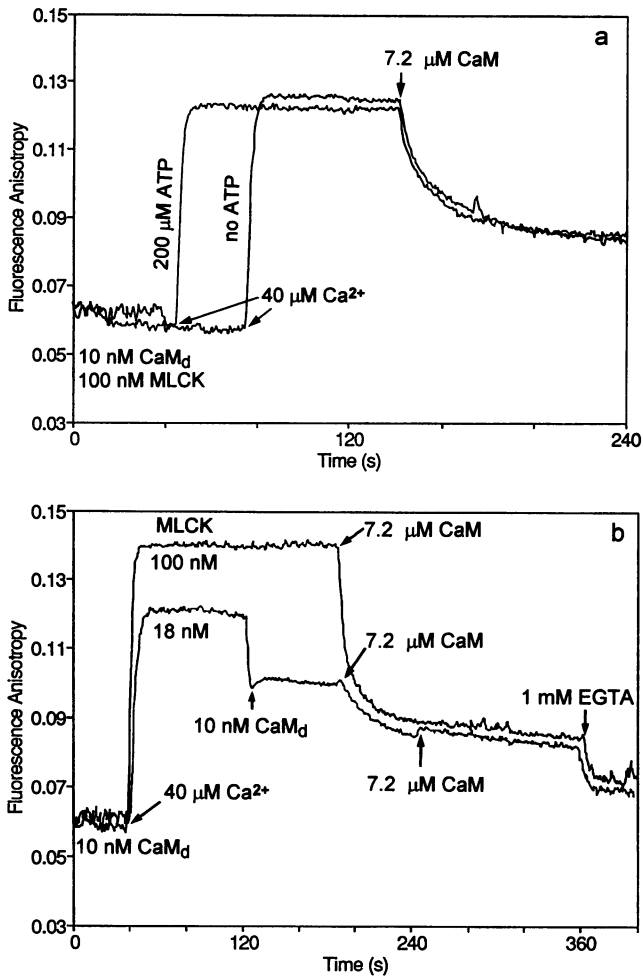

FIGURE 12 Fluorescence anisotropy changes of dansylated CaM-MLCK complex in the presence and absence of ATP (*a*), and at two different MLCK to CaM ratios (*b*), following addition of excess of unlabeled calmodulin. Excitation wavelength was 330 nm and that of fluorescence registration 510 nm.

(Fig. 12 *a*) so that the subsequent experiments could be done without ATP addition.

Fig. 12 *b* shows that the anisotropy decrease was 6 times faster when there was a 5-fold molar excess of MLCK over CaM in comparison to the case when MLCK and CaM were present at the same molar concentrations. Assuming that the "on" rate remained unchanged, this indicates that the affinity of MLCK for CaM in the presence of its high molar ratios was 6 times lower than when CaM and the kinase were at the same molar concentrations.

DISCUSSION

MLCK oligomeric suprastructure

It is generally known that enzymes function in the living cell by assembling into supramolecular structures such as dimers, tetramers, or larger polymers (for review see Schultz and Schirmer, 1979). Only recently the oligomer-

type allosteric effects have been demonstrated for a couple of CaM-dependent enzymes, namely skeletal muscle phosphofructokinase (Mayr and Helmeyer, 1983; Mayr, 1984 a, b) and erythrocyte Ca^{2+}-ATPase (Kosk-Kosicka et al., 1990). In most previous studies the smooth muscle MLCK has been assumed to be monomeric (Edelman et al., 1987; Hartshorne, 1987; Stull et al., 1993). By contrast, our previous conclusion was that MLCK is an oligomeric enzyme (see Sobieszek, 1991). The presence of dimers in MLCK solutions was first demonstrated by the method of ultracentrifugation (Ausio et al., 1992); the presence of hexamers was suggested earlier (see Sobieszek et al., 1991) and was used to explain the observed positive cooperativity of MLCK activation by CaM (Sobieszek, 1993; Sobieszek, 1994). In the investigation of Babiychuk et al. (1995), dimerization and oligomerization of turkey gizzard MLCK was demonstrated by SDS-PAGE combined with the zero-length cross-linkage method. In the present study we verify virtually for the first time, and by direct methods, the existence of three MLCK species, i.e., oligomers, dimers, and monomers. In our light-scattering measurements the emission from a red region was used. This emission brings about no changes to the protein system used. Therefore, the data obtained may be considered as very reliable.

According to our data, the MLCK dimer was 200 kDa, which is in good agreement with the 105.8 kDa calculated for the monomer by Olson et al. (1990) from the amino acid sequence. From analytical ultracentrifugation experiments, Ausio et al. (1992) concluded that the MLCK molecule is of rodlike shape, being 50 nm in length, 2.15 nm in diameter, and exhibiting a 14.4-nm RMS radius. According to their data, the RMS radius for the MLCK dimer should be ~24 nm, which agrees again with our 22 nm value (Table 4). Close in size is the heavy meromyosin subfragment 2 (SF2) with dimensions of 60×2 nm (Lowey et al., 1967). The hydrodynamic diameter of the SF2 was found by the PCS method to be 10.8 nm (Carlson and Fraser, 1974), which is close to our 8.8 nm D_{av} value for MLCK monomer (Table 1). Ausio et al. (1992) did not observe MLCK oligomers because their investigations were carried out at higher ionic strength conditions (0.2 M NaCl) together with additional high sucrose concentrations present. These factors reduce strongly ionic and hydrophobic interactions, which are normally responsible for this type of supramolecular assemblies.

It is important to point out that despite the 100-fold difference in the M_w of the oligomer, its RMS radius was only ~4 times larger than that of the dimer, i.e., 80 nm. This may be interpreted as indicating that the oligomer represents some kind of flexible spiral structure in which MLCK molecules associate in head-to-tail fashion, with the limiting configurations being a ring and a long rod. It can be shown (see also Wyatt, 1993) that for a spiral the RSM radius is equal to $R_g = \sqrt{\{R^2+(cN)^2/12\}} = \sqrt{\{R^2+H^2/12\}}$; where R, c, N, and H are radius, pitch, number of turns, and height of a spiral, respectively. The head-to-tail, and not head-to-head or tail-to-tail, association of MLCK molecules was concluded from the observations that the kinase was bound to cation and anion exchange gels. This is indicative of the two oppositely charged and well separated domains that participate in this head-to-tail association. However, we cannot exclude the possibility of a dimer being the basic unit, which then aggregates into the larger assemblies.

Inhibitory effect and MLCK activation by CaM

As we have previously shown (Sobieszek, 1991) almost complete inhibition of the kinase activity occurs after preincubation of the kinase at substoichiometric molar ratios to CaM. This inhibition was interpreted in terms of redistribution between different kinase forms (Sobieszek et al., 1993) taking place during the preincubation period before initiation of the activity measurements. In this report we show that the ratio between kinase species, characteristic for the apoenzyme, is still roughly maintained after its activation. Therefore, the observed MLCK inhibition cannot be explained by the redistribution of the kinase oligomeric forms. We cannot exclude 5 to 10% quantitative changes between dimer and monomer species, but this would not explain the almost complete inhibition of the enzyme. Our fluorescence data, which reflect changes of the protein chromophore environment, show that this inhibition, accompanied by a severalfold reduction of Ca^{2+} affinity for CaM-MLCK complex, correlates better with conformational changes of the kinase molecule.

It must be noted that the fluorescence methods we used give different information about conformational rearrangement of activated kinase. Indeed, probe 9AC binds to MLCK in the region of ATP binding and competes with ATP for this region (Malencik et al., 1982). As a consequence, 9AC fluorescence decrease indicates the reduction of the probe affinity (and, hence, ATP affinity) for the ATP binding site. This may arise from certain steric hindrances in the ATP binding site. As such they might have local character and may not be necessarily coupled with the reduction of CaM affinity for MLCK. However, changes of MLCK intrinsic tryptophanyl fluorescence during the preincubation period points directly to this latter possibility, which is explained below.

In the amino acid sequence of kinase there are four tryptophanyls (Knighton et al., 1992), three of which are in the region of the substrate binding site (residues 700, 733, and 773). Hydrophobic surroundings of these tryptophanyls (placed in the interior of the molecule) and their fluorescence characterized by a maximal short wavelength spectral shift should not practically change at a Ca^{2+}-CaM binding. The fourth tryptophanyl (Trp-800) is in the pseudosubstrate domain (residues 787–807) on the molecule surface (Knighton et al., 1992) and must therefore be characterized by a fluorescence spectrum with a maximum of ~340 nm (Burstein et al., 1973). Upon activation of the kinase, part of the pseudosubstrate domain, including this tryptophanyl, binds to Ca^{2+}-CaM. As a result, Trp-800 is covered by

CaM, which leads to a short wavelength shift of its fluorescence and to an increase of quantum yield (Burstein et al., 1973). As a consequence, the total fluorescence spectrum of the protein is shifted toward short wavelengths and its quantum yield is increased, as shown by Malencik et al. (1982). The decrease of intrinsic fluorescence of activated kinase during the preincubation period must therefore result from the increase of Trp-800 availability for a water environment, and it points directly to reduction of the MLCK affinity for CaM. Fluorescence anisotropy data obtained with dansylated CaM also point to the affinity reduction. This reduction must be the result of MLCK conformation changes that may be influenced by mutual positioning of kinase molecules or their fragments within the supramolecular structures.

Oligomerization and localization of MLCK

It is clear from the Fig. 6 *c* that the kinase oligomer exhibited virtually constant R_g for a very wide range of M_w (6×10^5-10^7). Therefore, the minimal oligomer must correspond to a hexamer (6×10^5). Furthermore, the increase in the M_w seen in the figure must result from aggregation of these hexamers to parallel structures because no significant increase in their RMS radii was observed. The structure of such a hexamer spiral is illustrated in Fig. 13 *a* with its R_g value accurately established, but its height (*H*) known only very approximately. This hexamer should fit the myosin filament helical structure deduced from the optical diffraction analysis of the negatively stained self-assembled filaments (Sobieszek, 1972; 1977) because exactly these same filaments bind MLCK with exceptionally high affinity (Sobieszek, 1990). The surface arrangement of myosin heads (on the filament core) for the myosin helix is shown in our model (Fig. 13 *b*). The model illustrates that the 258-nm long kinase spiral deduced from our light scattering data may be readily accommodated by the filament helical structure with 72 nm repeat and 108 nm pitch. With the filament diameter of ~18 nm (Xu et al., 1996) and 1 nm kinase radius the hexamer spiral diameter should also be approximately equal to 20 nm. The RMS radius of such a structure is 75 nm (i.e., $R_g = \sqrt{\{R^2+H^2/12\}}$) which is in agreement with the value obtained from our light scattering data.

It should be noted that the proposed model applies only to localization of MLCK under resting conditions, i.e., in absence of Ca^{2+} when CaM and the kinase are bound to the filament with high affinity and independent of each other (Sobieszek, 1990). During activation, the arrangement may change and this is known to be accompanied by reduction in the affinity of the active CaM-MLCK complex for myosin (Seller and Pato, 1984; Sobieszek, 1990). Further reduction takes place after phosphorylation of myosin and, as a result, the kinase can more readily be translocated to phosphorylate other myosin heads on the filament surface. We believe that CaM binding proteins associated with thin filaments such as caldesmon and calponin may participate in this translocation process.

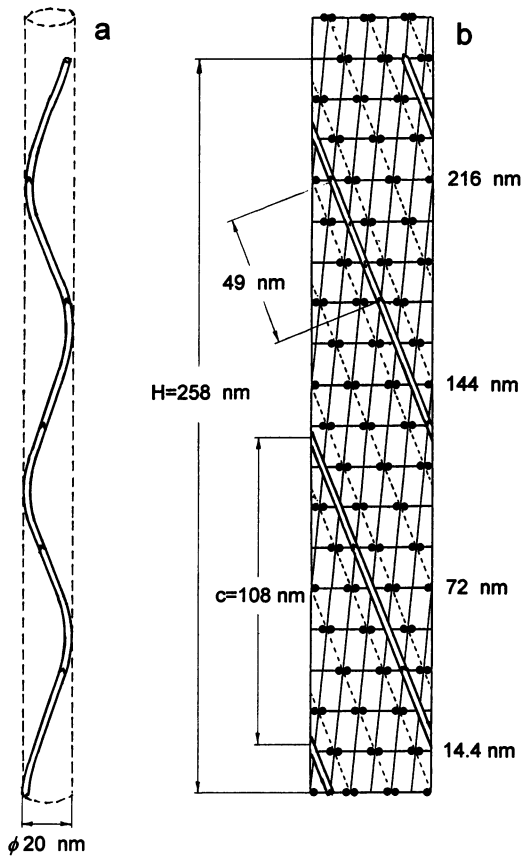

FIGURE 13 Deduced spiral-like structure of MLCK hexamer (*a*) and its possible relationship to the helical structure of self-assembled myosin filaments (*b*) taken from Sobieszek (1977). For more details see text.

We thank Dr. Tobias Meyer of the Department of Cell Biology at Duke University Medical Center (Durham, NC) for his assistance with the fluorescence anisotropy experiments, and Dr. Christoph Johann for his free loan of a Wyatt Technology multi-angle laser light scattering instrument and discussions. We also thank Ms. Margot Sluka for grammar corrections to the manuscript.

This work was supported by grants from the Austrian Science Foundation and from the East-West Program of the Austrian Ministry for Science and Research (to A.S.).

REFERENCES

Adelstein, R. S., and E. Eisenberg. 1980. Regulation and kinetics of the actin-myosin-ATP interaction. *Annu. Rev. Biochem.* 19:921–956.

Adelstein, R. S., and C. B. Klee. 1981. Purification and characterization of smooth muscle myosin light chain kinase. *J. Biol. Chem.* 256: 7501–7509.

Ausio, J., D. A. Malencik, and S. R. Anderson. 1992. Analytical sedimentation studies of turkey gizzard myosin light chain kinase. *Biophys. J.* 61:1656–1663.

Babiychuk, E. B., V. S. Babiychuk, and A. Sobieszek. 1995. Modulation of smooth muscle myosin light chain kinase activity by Ca^{2+}-calmodulin dependent, oligomeric-type modifications. *Biochemistry.* 34: 6366–6372.

Braginskaya, T. G., P. D. Dobichin, and M. A. Ivanova. 1983. Analysis of the polydispersity by photon correlation spectroscopy. *Physica Scripta.* 26:309–315.

Burstein, E. A., N. S. Vedenkina, and M. N. Ivkova. 1973. Fluorescence and the location of tryptophan residues in protein molecules. *Photochem. Photobiol.* 18:263–271.

Carlson, F. D., and A. B. Fraser. 1974. Intensity fluctuation autocorrelation studies of the dynamics of muscular contraction. *In* Photon Correlation and Light Beating Spectroscopy. H. Z. Cummins and E. R. Pike, editors. Plenum Press, New York. 519–532.

Edelman, A. M., D. K. Blumenthal, and E. G. Krebs. 1987. Protein serine/threonine kinases. *Annu. Rev. Biochem.* 56:567–613.

Gornall, A. G., C. J. Bardawill, and M. M. David. 1949. Determination of serum proteins by means of the biuret reaction. *J. Biol. Chem.* 177: 751–766.

Hartshorne, D. J. 1987. Biochemistry of the contractile process in smooth muscle. *In* Physiology of the Gastrointestinal Tract, 2nd ed., Vol. 1. L. A. Johnson, editor. Raven Press, New York. 423–481.

Hartshorne, D. J., and T. Kawamura. 1992. Regulation of contraction-relaxation in smooth muscle. *NIPS.* 7:59–64.

Ikebe, M., S. Maruta, and S. Reardon. 1989. Location of the inhibitory region of smooth muscle myosin light chain kinase. *J. Biol. Chem.* 256:6967–6971.

Ikebe, M., M. Stepinska, B. E. Kemp, A. R. Means, and D. J. Hartshorne. 1987. Proteolysis of smooth muscle myosin light chain kinase. Formation of inactive and calmodulin-independent fragments. *J. Biol. Chem.* 262:13828–13834.

Ikura, M., G. M. Clore, A. M. Gronenborn, G. Zhu, C. B. Klee, and Z. Bax. 1992. Solution structure of a calmodulin-target peptide of smooth muscle myosin light chain kinase. *Science.* 256:632–638.

Ito, M., V. Guerriero, Jr., X. Chen, and D. J. Hartshorne. 1991. Determination of the inhibitory domain of smooth muscle myosin light chain kinase by site directed mutagenesis. *Biochemistry.* 30:3498–3503.

Kamm, K. E., and J. T. Stull. 1985. The function of myosin and myosin light chain phosphorylation in smooth muscle. *Annu. Rev. Pharmacol. Toxicol.* 25:593–620.

Kemp, B. E., R. B. Pearson, V. Guerriero, Jr., J. C. Bagchi, and A. R. Means. 1987. The calmodulin binding domain of chicken smooth muscle myosin light chain kinase contains a pseudosubstrate sequence. *J. Biol. Chem.* 262:2542–2548.

Kennelly, P. J., A. M. Edelman, D. K. Blumenthal, and E. G. Krebs. 1987. Rabbit skeletal muscle myosin light chain kinase. The calmodulin binding domain as a potential active site-directed inhibitory domain. *J. Biol. Chem.* 262:11958–11963.

Knighton, D. R., R. B. Pearson, J. M. Sowadski, A. R. Means, L. F. T. Eyck, S. S. Taylor, and B. E. Kemp. 1992. Structural bases of the intrasteric regulation of myosin light chain kinases. *Science.* 258: 130–135.

Kosk-Kosicka, D., T. Bzdega, A. Wawrzynow, S. Scaillet, K. Nemcek, and J. D. Johnson. 1990. Erythrocyte Ca^{2+}-ATPase: activation by enzyme oligomerization versus by calmodulin. *In* Calcium Binding Proteins in Normal and Transformed Cells. R. Pochet, D. Eric, M. Lawson, and C. W. Heizmann, editors. Plenum Publishing Corporation New York. 169–174.

Lowey, S., L. Goldstein, C. Cohen, and S. M. Luck. 1967. Proteolytic degradation of myosin and the meromyosins by a water-insoluble polyanionic derivative of trypsin. Properties of a helical subunit isolated from heavy meromyosin. *J. Mol. Biol.* 23:287–307.

Malencik, D. A., S. R. Anderson, J. L. Bohnert, and Y. Shalitin. 1982. Functional interactions between smooth muscle myosin light chain kinase and calmodulin. *Biochemistry.* 21:4031–4039.

Marston, S. B. 1982. The regulation of smooth muscle contractile proteins. *Progr. Biophys. Mol. Biol.* 41:1–41.

Mayr, G. W. 1984a. Interaction of calmodulin with muscle phosphofructokinase. Changes of the aggregation state, conformation and catalytic activity. *Eur. J. Biochem.* 143:513–520.

Mayr, G. W. 1984b. Interaction of calmodulin with muscle phosphofructokinase: interplay with metabolic effectors of the enzyme under physiological conditions. *Eur. J. Biochem.* 143:521–529.

Mayr, G. W., and L. M. J. Heilmeyer, Jr. 1983. Skeletal muscle myosin light chain kinase. A refined structural model. *FEBS Lett.* 157:225–231.

Meador, W. E., A. R. Means, and F. A. Quiocho. 1992. Target enzyme recognition by calmodulin: 2.4 Å structure of a calmodulin-peptide complex. *Science.* 257:1251–1255.

Means, A. R., I. C. Bagchi, M. F. A. VanBerkum, and B. E. Kemp. 1991. Regulation of smooth muscle myosin light chain kinase by calmodulin. *In* Regulation of Smooth Muscle Contraction. R. S. Moreland, editor. Plenum Press, New York. 11–24.

Meyer, T., P. I. Hanson, L. Stryer, and H. Schulman. 1992. Calmodulin trapping by calcium-calmodulin-dependent protein kinase. *Science.* 256: 1199–1202.

Nicoli, D. F., D. C. McKenzie, and J.-S. Wu. 1992. Application of dynamic light scattering to particle size analysis of macromolecules. *International Laboratory.* 24:32–37.

Olson, N. J., R. B. Pearson, D. S. Needleman, M. Y. Hurwitz, B. E. Kemp, and A. R. Means. 1990. Regulatory and structural motifs of chicken gizzard myosin light chain kinase. *Proc. Natl. Acad. Sci. USA* 87: 2284–2288.

Pearson, R. B., M. Ito, N. A. Morrice, A. J. Smith, R. Condron, R. E. H. Wettenhall, B. E. Kemp, and D. J. Hartshorne. 1991. Proteolytic cleavage sites in smooth muscle myosin light chain kinase and their relations to structural and regulatory domains. *Eur. J. Biochem.* 200:723–730.

Pearson, R. B., E. H. Wettenhall, A. R. Means, D. J. Hartshorne, and B. E. Kemp. 1988. Autoregulation of enzymes by pseudosubstrate prototypes: myosin light chain kinase. *Science.* 241:970–973.

Perrie, W. T., and S. V. Perry. 1970. An electrophoretic study of the low-molecular-weight components of myosin. *Biochem. J.* 119:31–38.

Schulz, G. E., and R. H. Schirmer. 1979. Principles of Protein Structure. Springer-Verlag, New-York.

Sellers, J. R., and M. O. Pato. 1985. The binding of smooth muscle myosin light chain kinase and phosphatase to actin and myosin. *J. Biol. Chem.* 259:7740–7746.

Small, J. V., and A. Sobieszek. 1980. The contractile apparatus of smooth muscle. *Int. Rev. Cytol.* 64:241–306.

Sobieszek, A. 1972. Cross-bridges on self-assembled smooth muscle myosin filaments. *J. Mol. Biol.* 70:741–744.

Sobieszek, A. 1977. Vertebrate smooth muscle myosin: enzymatic and structural properties. *In* The Biochemistry of Smooth Muscle. N. L. Stephens, editor. University Park Press, Baltimore. 413–443.

Sobieszek, A. 1985. Phosphorylation reaction of vertebrate smooth muscle myosin: an enzyme kinetic analysis. *Biochemistry.* 29:1266–1274.

Sobieszek, A. 1988. Bulk isolation of the 20,000-Da light chain of smooth muscle myosin: separation of the unphosphorylated and phosphorylated species. *Anal. Biochem.* 172:43–50.

Sobieszek, A. 1990. Smooth muscle myosin as a calmodulin binding protein. Affinity increase on filament assembly. *J. Muscle Res. Cell Motil.* 11:114–124.

Sobieszek, A. 1991. Regulation of smooth muscle myosin light chain kinase. Allosteric effects and co-operative activation by calmodulin. *J. Mol. Biol.* 220:947–957.

Sobieszek, A. 1994. Regulation of myosin light chain kinase: kinetic mechanism, autophosphorylation, and cooperative activation by Ca^{2+} and calmodulin. *Can. J. Physiol. Pharmacol.* 72:1368–1376.

Sobieszek, A., and B. Barylko. 1984. Enzymes regulating myosin phosphorylation in vertebrate smooth muscle. *In* Smooth Muscle Contraction. N. L. Stephens, editor. Marcel Dekker, New York. 283–316.

Sobieszek, A., and R. D. Bremel. 1975. Preparation and properties of vertebrate smooth muscle myofibrils and actomyosin. *Eur. J. Biochem.* 55:49–60.

Sobieszek, A., A. Strobl, B. Ortner, and E. Babiychuk. 1993. Ca^{2+}-calmodulin-dependent modification of smooth-muscle myosin light chain kinase leading to its co-operative activation by calmodulin. *Biochem. J.* 295:405–411.

Stull, J. T., M. G. Tansey, D.-C. Tang, R. A. Word, and K. E. Kamm. 1993. Phosphorylation of myosin light chain kinase: a cellular mechanism for Ca^{2+} desensitization. *Mol. Cell. Biochem.* 127/128:229–237.

Tanaka, M., R. Ikebe, M. Matsuura, and M. Ikebe. 1995. Pseudosubstrate sequence may not be critical for autoinhibition of smooth muscle myosin light chain kinase. *EMBO J.* 14:2839–2846.

VanBercum, M. F. A., and A. R. Means. 1991. Three amino acid substitutions on domain I of calmodulin prevent the activation of chicken smooth muscle myosin light chain kinase. *J. Biol. Chem.* 266: 21488–21495.

Williams, D. A., and F. S. Fay. 1986. Calcium transients and resting levels in isolated smooth muscle cells monitored with quin 2. *Am. J. Physiol.* 250:C779–C791.

Wyatt, P. J. 1993. Light scattering and absolute characterization of macromolecules. *Analitica Chimica Acta.* 272:1–40.

Xu, J.-Q., B. A. Harder, P. Uman, and R. Craig. 1996. Myosin filament structure in vertebrate smooth muscle. *J. Cell Biol.* 134:53–66.

Yano, K., Y. Araki, S. J. Hales, M. Tanaka, and M. Ikebe. 1993. Boundary of the autoinhibitory region of smooth muscle myosin light-chain kinase. *Biochemistry.* 32:12054–12061.